Supplementary Information
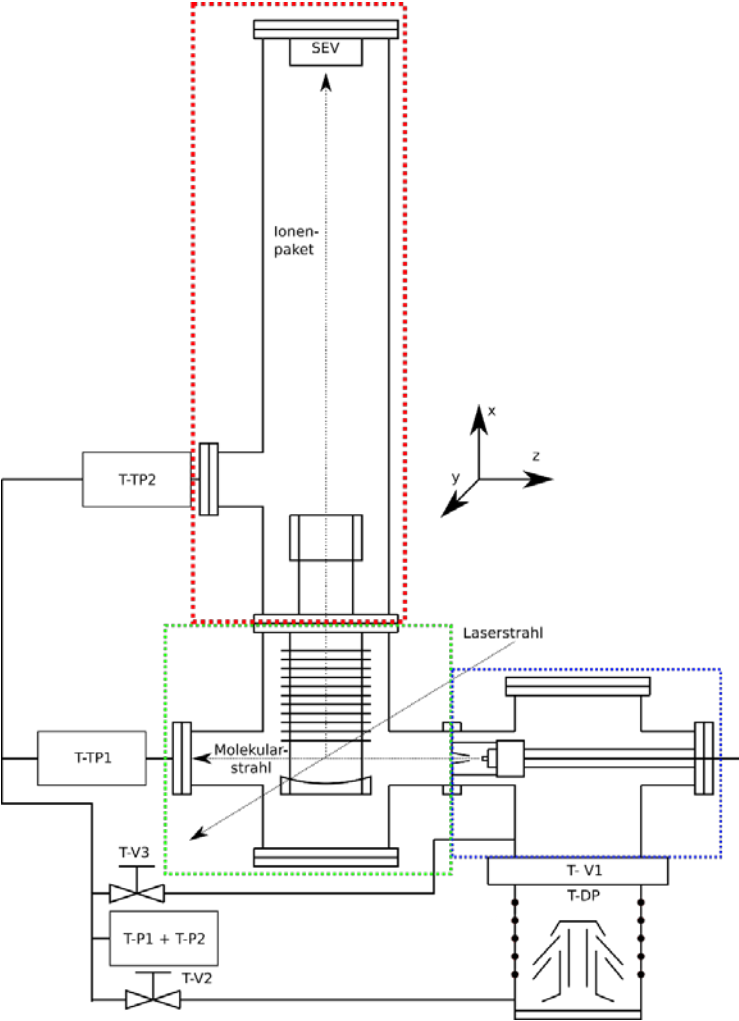
Photodissociation of deuterated pyrrole-ammonia clusters: H-atom transfer or electron coupled proton transfer?

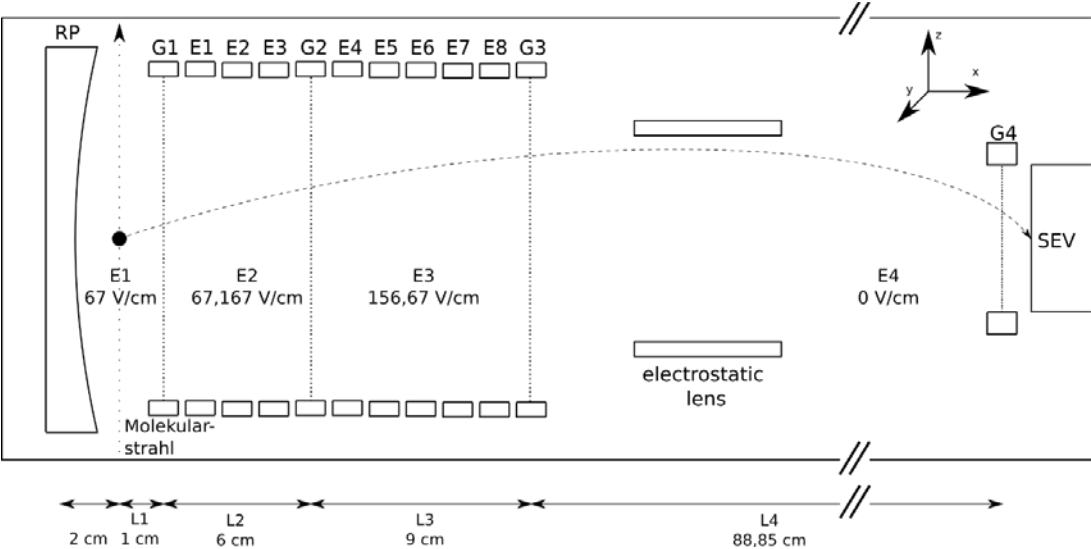*Stefan Fuchs and Bernhard Dick**

Institut für Physikalische und Theoretische Chemie, Universität Regensburg,
Universitätsstraße 31, 93053 Regensburg

Table of content: page

Design of the TOF apparatus

Detail of the electrode arrangement in the TOF accelerator and drift tube.

Figure S2
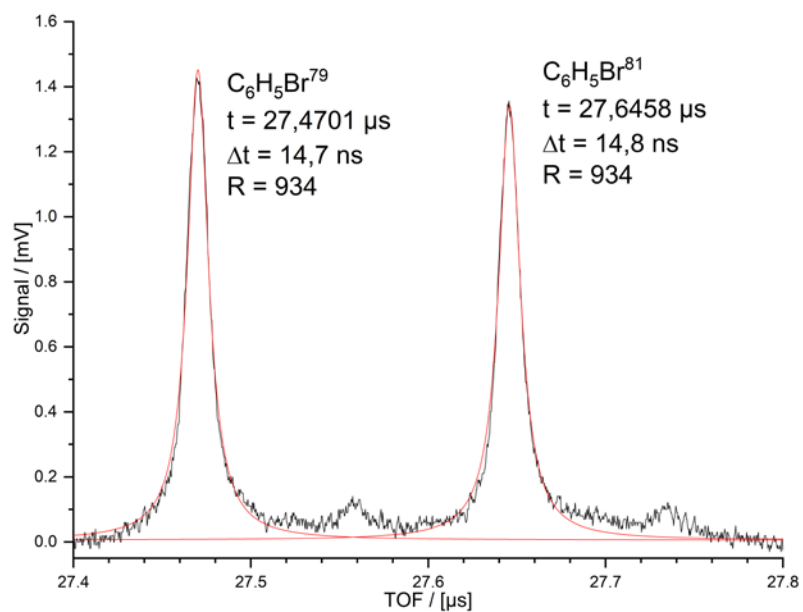

Figure S2: TOF signal of bromobenzene. The two isotopic peaks are fitted by Gaussians. The calculated mass resolution m/Δm of 934 is limited by the rise time of the detector and the pulse duration of the ionization laser.

A short description of MEVELER and MELEXIR.

Following the request of one of the referees I give here a short summary of the philosophy behind the methods MEVELER and MELEXIR.

The three-dimensional (3D) velocity distribution of photofragments (or photoelectrons) can – in the initial inertial frame – be expressed either as a function in cartesian or in spherical coordinates:

$$P(v, \vartheta, \varphi)\, v^2 dv \sin(\vartheta)\, d\vartheta\, d\varphi = \tilde{P}(x, y, z)\, dx\, dy\, dz \tag{1}$$

where eq. 1 also shows the volume element for integration. A VMI (velocity map imaging) experiment measures the projection of this distribution onto a planar detector, which can be written as the integral of the distribution function in cartesian coordinates along one axis:

$$B(z, x) = \int_{-\infty}^{\infty} \tilde{P}(x, y, z)\, dy \tag{1}$$

Transforming the right side to spherical coordinates results in a rather involved expression. When the velocity distribution is rotationally symmetric around the z-axis, which is the case when the process is initiated by linearly polarized light, the projection $B(z, x)$ contains the full information about the velocity distribution. In this case the integral of eq. 2 is called the Abel transform.

Although a mathematical expression for the inversion of the Abel transform exists, application of this inverse Abel transform to noisy data can result in very large artifacts, e.g. negative intensities. The reason is that this inversion belongs to the class of ill-posed problems, similar to the inversion of a singular matrix.

Many algorithms have been designed to cope with this problem, and most of these involve processing of the data like smoothing. The maximum entropy philosophy, however, allows to treat this problem without ever using any inverse transform. Instead, it applies the stable forward transform to the 2D distribution $U(v, \vartheta)$ and compares the result to the experimental data $B(z, x)$. The agreements is measured by the so-called likelihood L which, in the case of Gaussian noise, is given by the sum of square deviations. A similar criterion can be formulated for Poissonian noise, which is the proper form for counting events.

Best agreement with the data is obtained by minimizing this likelihood function through iterative variation of $U(v, \vartheta)$. However, we have the same number of unknowns (pixels in $U(v, \vartheta)$) as the number of data points (pixels in in $B(z, x)$). Therefore, a huge number of solutions with the same value of the likelihood exists.

The maximum entropy method selects from these solutions the one with the smallest information content, which is measured by the configurational entropy. In other words, all other solutions contain more information than necessary to explain the data, i.e., for which there is no evidence in the data. Computationally, this is a constrained optimization problem.

The maximum entropy idea can be applied to the full data set without assuming anything about the original velocity distribution function. I have called this method MEVIR, for **M**aximum **E**ntropy **V**elocity **I**mage **R**econstruction. However, frequently the experimental process imposes some constraints on the velocity distribution which can be used as prior knowledge in the analysis. When the process is initiated by one-photon absorption via a dipole transition, the expected form of the distribution is

$$U(v, \vartheta) = \frac{1}{2}\, p(v)[1 + \beta(v)\, P_2(\cos \vartheta)] \tag{3}$$

Where integration over the angle φ has already been performed. Most researchers consider the anisotropy parameter β as a single constant, but more correctly it should be considered a function of the velocity.

Since $\beta(v)$ is ill-defined at velocities where $p(v)$ vanishes, I use the following representation inside the ME programs:

$$U(v,\vartheta) = \frac{1}{v^2} \sum_{l=0}^{k} Q_l(v)\ P_1(\cos\vartheta) \tag{4}$$

When the sum is restricted to l=0 and l=2, this expression is equivalent to eq. 3, i.e.

$$Q_0(v) = \int_0^\pi U(v,\vartheta)\ v^2 \sin(\vartheta)\ d\vartheta = v^2\ p(v) \tag{5}$$

And the anisotropic part is

$$Q_2(v) = v^2\ p(v)\ \beta(v) \tag{6}$$

The program MEVELER (**M**aximum **E**ntropy **VE**locity **LE**grendre **R**econstruction) [1] uses the expansion of eq. 4 with l restricted to l=0 and l=2. In each iteration, the full data set is predicted from the functions $Q_l(v)$ and compared to the actual experimental data with the Poissonian likelihood estimator. This uses the correct statistics, which is important when each pixel in the data set contains only a small number of counts.

For application of the program MELEXIR (**M**aximum **E**ntropy **L**egendre **EX**pansion **I**mage **R**econstruction)[2] the experimental data are first transformed to a representation as expansion in Legendre polynomials similar to eq. 4, which has been proposed by Harrison et al..

$$B(r,\alpha) = \frac{1}{r} \sum_{j=0}^{\infty} A_j(r)\ P_j(\cos\alpha) \tag{7}$$

Where r and α are the polar coordinates of the data point in the image $B(z,x)$.

Note that this is **not** a manipulation of the data because the transformation between these two representations is fully reversible. The key is that in the new representation only the Legendre projections $A_j(r)$ with $j \le l$ contribute to the solution $Q_l(v)$. Presently, MELEXIR can handle distributions up to l=6 (i.e. three photon events) and also odd values of l (i.e. orientation).

For readers interested in using these programs I include the program manual in the SI.

[1] B. Dick, Phys. Chem. Chem. Phys., 16 (2014) 470.

[2] B. Dick, Phys. Chem. Chem. Phys., 21 (2019) 19499.

[3] G. R. Harrison, J. C. Vaughan, B. Hidle and G. M. Laurent, J. Chem. Phys., 2018, 148, 194101.

On the next page, the performance of MELEXIR with sparse data is shown as an example. Mock data sets were generated by random sampling from a distribution with four velocity components. The reconstruction is still acceptable with 3600 counts, i.e. 0.01 counts per pixel in the image, whereas no structure is visible to the naked eye on the original image.

Performance of MELEXIR: left column: Mock images, generated by random sampling from a distribution of 4 velocity components. Right column: velocity distribution reconstructed with MELEXIR.
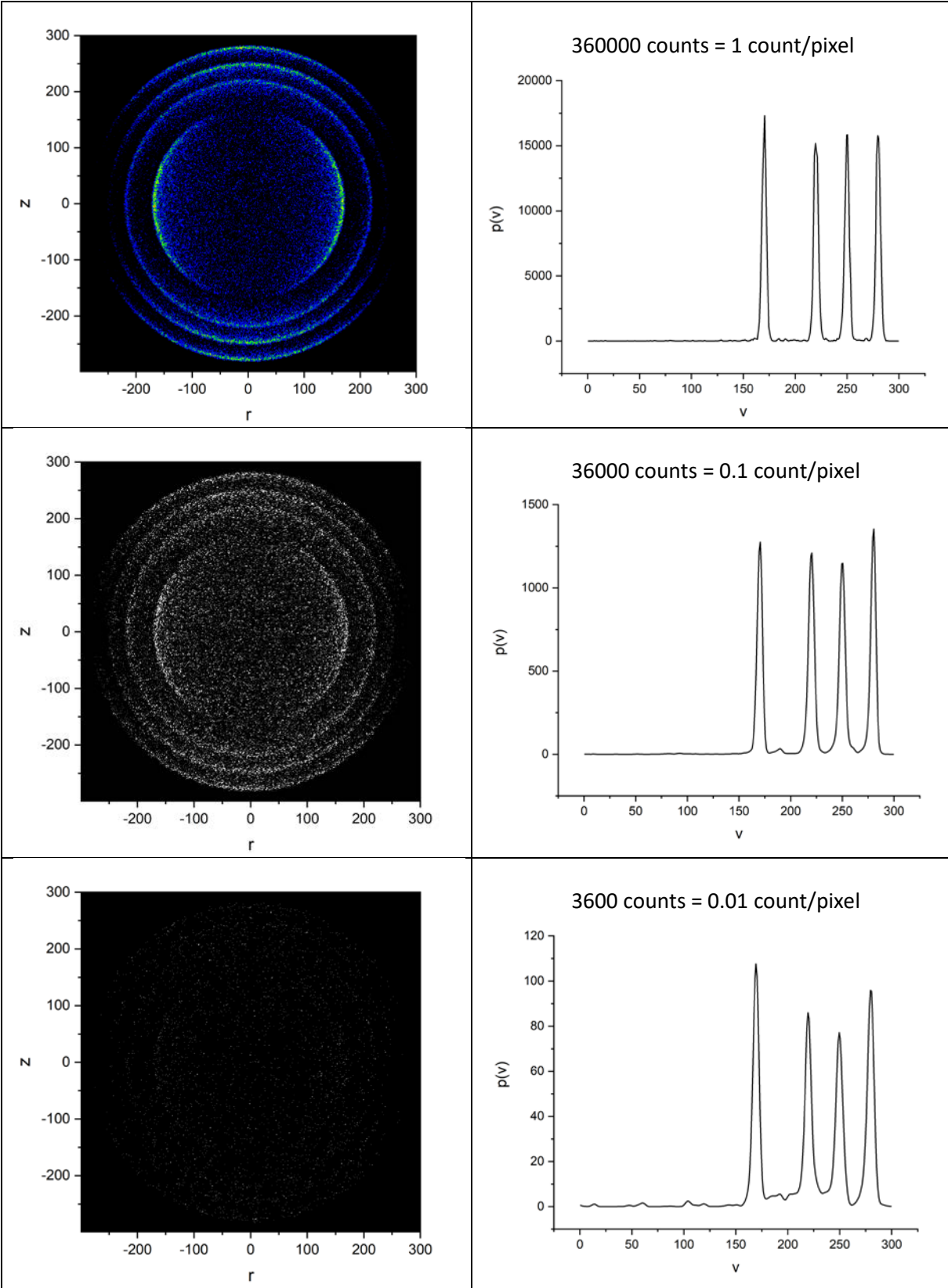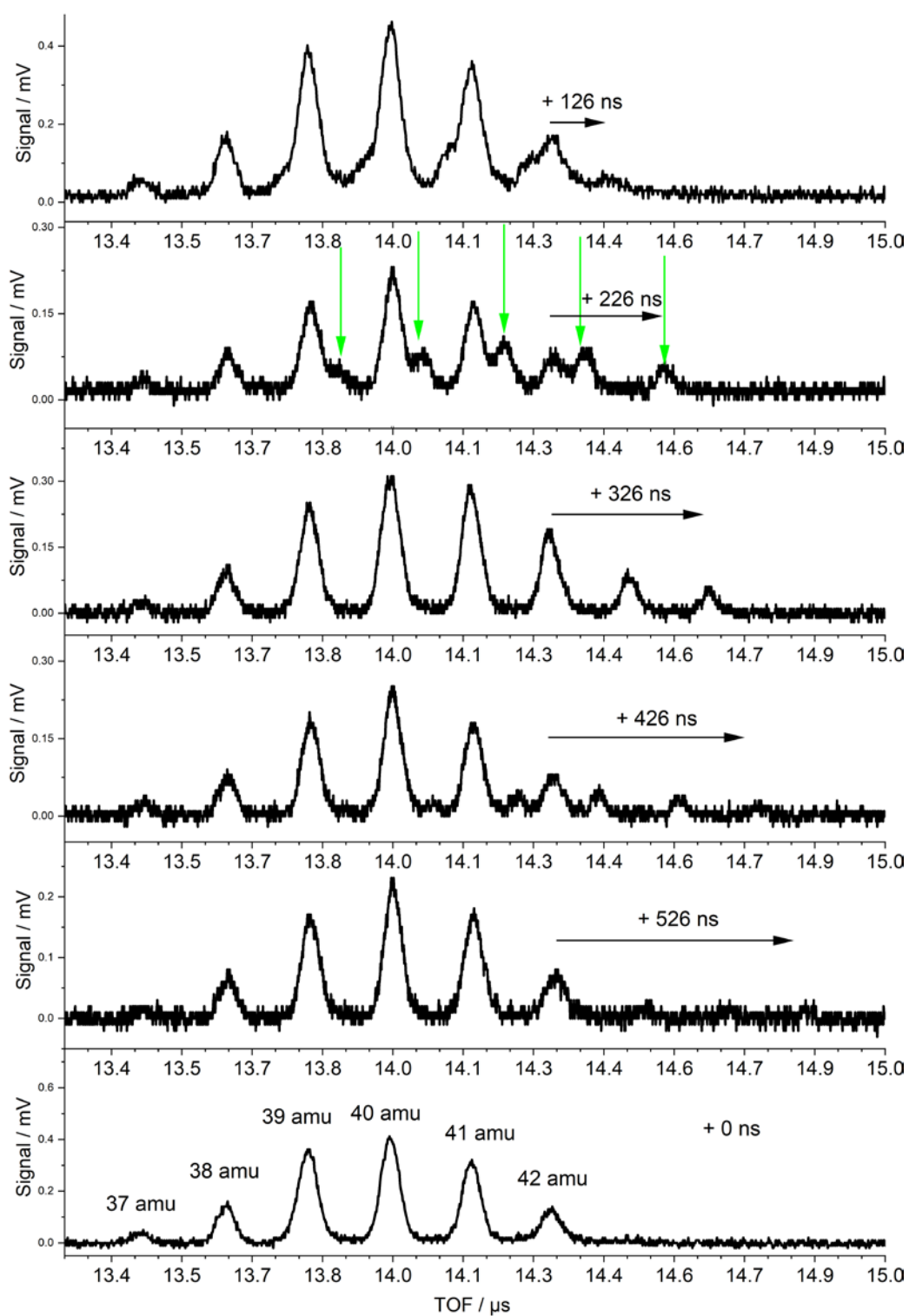
TOF spectra of the isotopomers of $ND_4(ND_3)$ obtained by 226 nm excitation of $PyH^*(ND_3)_2$ and delayed ionization with 266 nm photons at delay times indicated in each panel. Delayed signals are obtained for isotopomers containing up to 4 hydrogen atoms (see green arraows), indicating that these do not decompose quickly by tunneling.

Fig. S4: Ion Images for figure 6

Ion image of the "instantaneous" ND_4 cations, generated by excitation with 226 nm photons
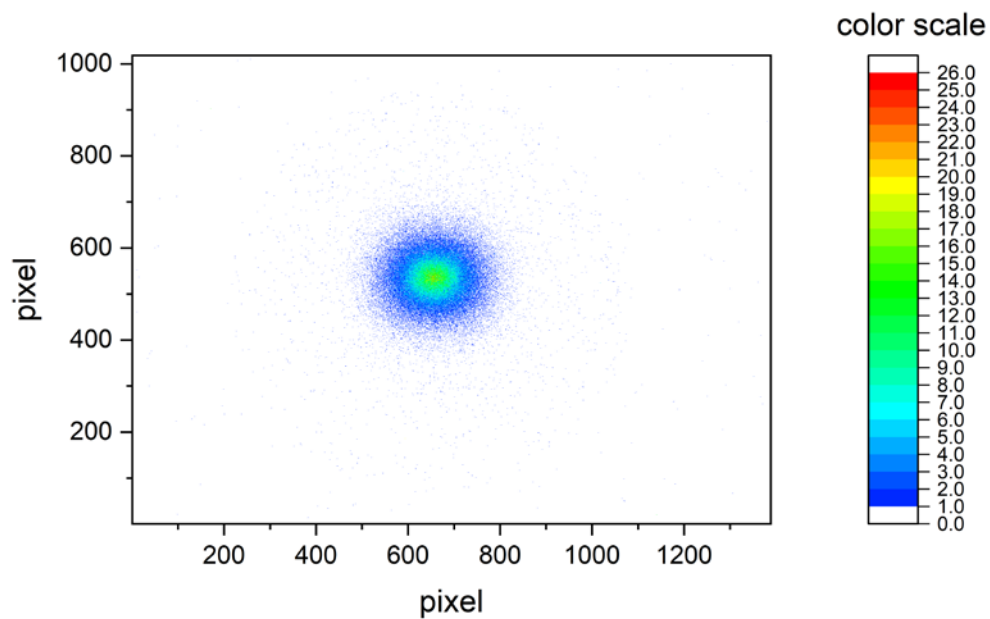
Ion image of the "delayed" ND_4 cations, generated by ionization with 266 nm photons 300 ns after excitation with 226 nm photons.
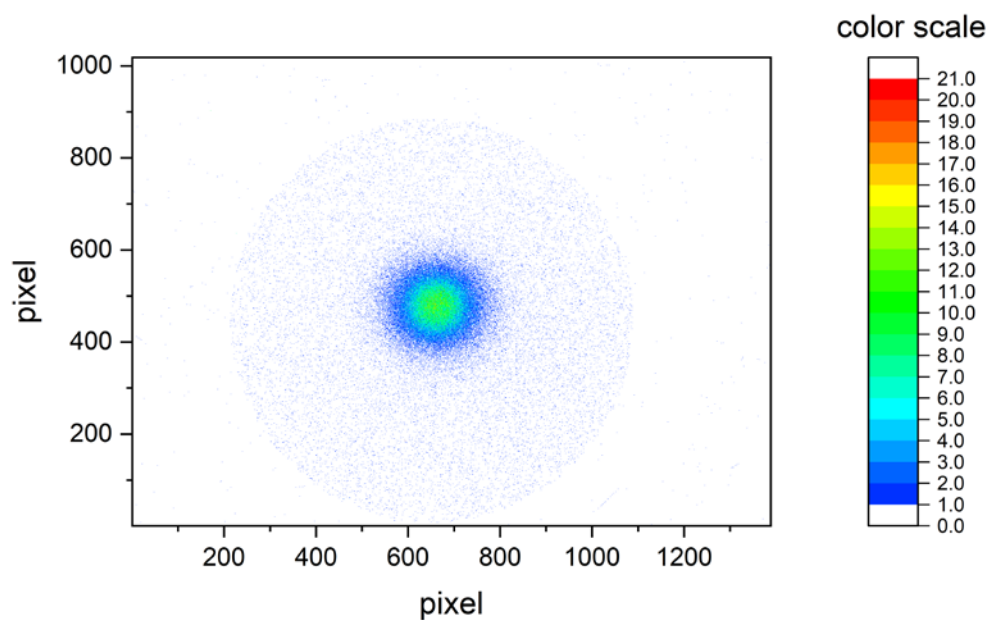
Extended basis set for nitrogen atoms

ORCA:

```
%basis
 NewGTO 7 # new basis for nitrogen
 "cc-pVTZ"
 S  1
 1    0.576000000E-01    1.00000000
 S  1
 1    0.288000000E-01    1.00000000
 P  1
 1    0.491000000E-01    1.00000000
 P  1
 1    0.245500000E-01    1.00000000
 end
end
```

Firefly / PCGAMESS

```
S  8
 1    11420.00000    0.5230000000E-03
 2    1712.000000    0.4045000000E-02
 3    389.3000000    0.2077500000E-01
 4    110.0000000    0.8072700000E-01
 5    35.57000000    0.2330740000
 6    12.54000000    0.4335010000
 7    4.644000000    0.3474720000
 8    0.5118000000   -0.8508000000E-02
 S  8
 1    11420.00000   -0.1150000000E-03
 2    1712.000000   -0.8950000000E-03
 3    389.3000000   -0.4624000000E-02
 4    110.0000000   -0.1852800000E-01
 5    35.57000000   -0.5733900000E-01
 6    12.54000000   -0.1320760000
 7    4.644000000   -0.1725100000
 8    0.5118000000    0.5999440000
 S  1
 1    1.293000000     1.000000000
 S  1
 1    0.1787000000    1.000000000
 P  3
 1    26.63000000    0.1467000000E-01
 2    5.948000000    0.9176400000E-01
 3    1.742000000    0.2986830000
 P  1
 1    0.5550000000    1.000000000
 P  1
 1    0.1725000000    1.000000000
 D  1
 1    1.654000000     1.000000000
 D  1
 1    0.4690000000    1.000000000
```

```
F  1
 1      1.093000000        1.000000000
S  1
 1     0.576000000E-01    1.00000000
S  1
 1     0.288000000E-01    1.00000000
P  1
 1     0.491000000E-01    1.00000000
P  1
 1     0.245500000E-01    1.00000000
```

Test calculations on NH_4 radical

Basis-set	Energy / H	N(basis)
cc-pVTZ	-56.681228	95
aug-cc-pVTZ (N only)	-56.702219	115
aug-cc-pVTZ (all atoms)	-56.712492	155
cc-pVTZ(+) (N only)	-56.712182	103
cc-pVTZ(+) (all atoms)	-56.712384	111

Table T1: Energy (in Harree units) of the NH_4 radical, calculated with different basis sets and ROHF wavefunction (Firefly program)

The cc-pVTZ(+) basis contains the functions of the cc-pVTZ basis plus the diffuse s-orbital from the aug-cc-pVTZ basis plus a further s-orbital with half the exponent.

Using the cc-pVTZ(+) basis on the N atom only improves the energy by 10 mH compared to the aug-cc-pVTZ basis on the N-atom. Using aug-cc-pVTZ on all atoms produces an additional improvement of only 0.3 mH at the cost of a 50% increase in the number of basis functions.
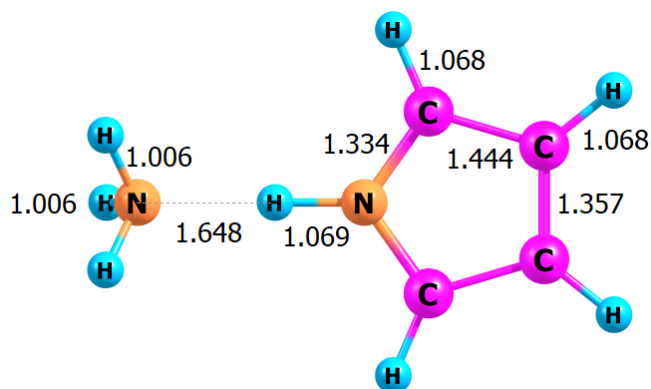
Optimized structures CASSCF(8|7)-XMCQDPT2/cc-pVTZ(+)
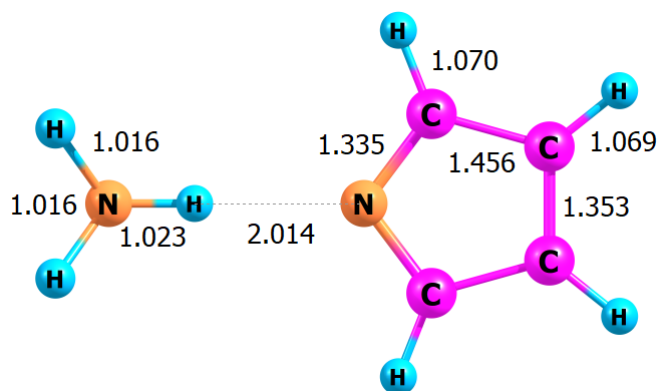
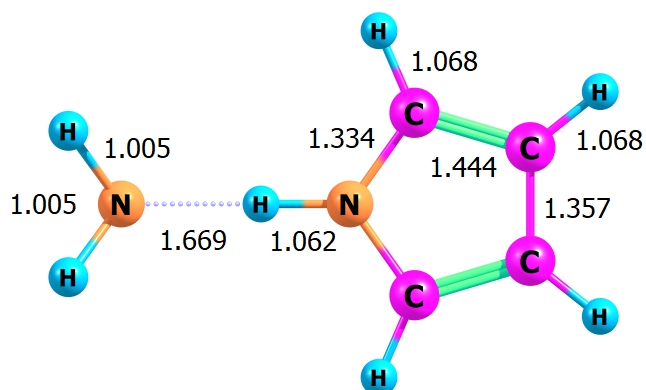## S0 minimum
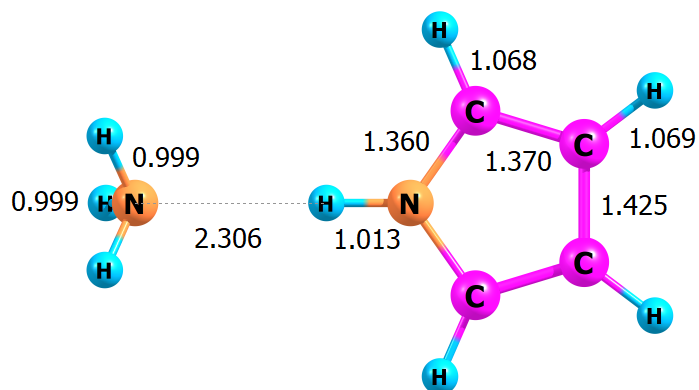
Dipole moment 4.25 Debye

S1-local minimum

Dipole moment 9.91 Debye
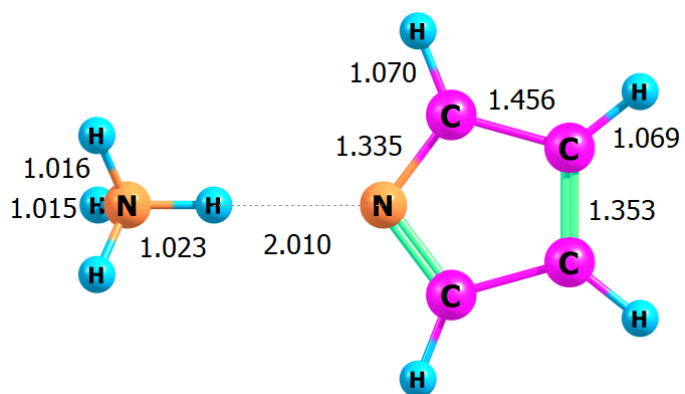
S1 – global minimum

Dipole moment 7.14 Debe

T1 – local minimum

Dipole moment 9.10 Debye

T1 – global minimum

Dipole moment 7.10 Debye